5

Regional-scale estimates of forest CO_2 and isotope flux based on monthly CO_2 budgets of the atmospheric boundary layer

Brent R. Helliker, Joseph A. Berry, Alan K. Betts, Peter S. Bakwin, Kenneth J. Davis, James R. Ehleringer, Martha P. Butler and Daniel M. Ricciuto

1. Introduction

Several lines of evidence point to persistent net annual carbon uptake and storage in the temperate latitudes of the Northern Hemisphere (Battle *et al.*, 2000; Bousqet *et al.*, 1999; Ciais *et al.*, 1995; Prentice *et al.*, 2001; Rayner *et al.*, 1999). This large carbon sink is thought to be largely in the northern forests (Goodale *et al.*, 2002; Chapter 8, this volume), although the tropical forest may also represent a substantial sink (Townsend *et al.*, 2002; Chapter 10, this volume). The uncertainties around these sinks are large (Bousqet *et al.*, 1999) and hypotheses concerning their location and mechanism vary (Bousqet *et al.*, 1999; Fan *et al.*, 1998; Rayner *et al.*, 1999; Chapter 2, this volume). Furthermore, the sustainability of these sinks, or the sustained remediation of anthropogenically derived atmospheric CO_2 by forest, is also a point of disagreement (Oren *et al.*, 2001). Considering the global expanse of forests, the importance of forests in the annual global carbon cycle and the uncertainty surrounding the size, duration and location of the northern hemisphere sink, it is imperative that we gain an understanding of forest productivity on large spatial and temporal scales (see Chapter 1, this volume).

The Carbon Balance of Forest Biomes, edited by H. Griffiths and P.G. Jarvis.

Studies of forest productivity have typically relied on stand-scale eddy covariance (EC) measurements or forest inventories (Baldocchi *et al.*, 2001; Goodale *et al.*, 2002). Together, these methodologies are invaluable in assessing changes in forest productivity in response to climate variability, longer-term climate change, and anthropogenic disturbance. EC measurements are ideal for observations of year-to-year variation in productivity. However, this method offers a relatively limited picture of forest productivity because the surface area of integration, or footprint, is typically less than 1 km^2. Additionally, heterogeneity at larger spatial scales often precludes the extrapolation of smaller scale measurements to larger scales. Forest inventories provide robust estimates of long-term productivity, but the time-scale of robust forest inventories is typically decadal, not annual (Goodale *et al.*, 2002; Chapter 3, this volume). In this chapter we outline the framework for the measurement of net CO_2 flux over large spatial (10^4–10^6 km^2) and temporal (months to years) scales through the ABL. This framework rests on the ABL-equilibrium assumption first developed through model approaches by Betts and Ridgway (1989) for the oceans, and extended to land by Betts (2000), Betts *et al.*, (2004) and for observation-based approaches by Helliker *et al.* (2004; see also Chapter 6, this volume). In this synthesis, we describe the application of the ABL equilibrium concepts to net CO_2 flux over land, and we extend these concepts to the stable isotopes of CO_2 measured in the ABL and the overlying free troposphere. The study area of interest is a temperate mixed-forest region in north-central Wisconsin, USA.

2. Atmospheric boundary layer description, scalar dynamics, and the equilibrium assumption

The ABL extends upwards from the Earth's surface about 1–2 km and is separated from the stable overlying free troposphere (which extends upwards an additional 8–9 km) by an inversion. The ABL is most distinct from the free troposphere when high-pressure systems persist and large-scale subsidence pushes free-tropospheric air down onto the ABL, and ABL air diverges horizontally. During these periods, the ABL is defined as the air mass below the capping inversion and, depending on the time of day, may include the daytime CBL, the nocturnal boundary layer and the residual boundary layer (Stull, 1988). During the day, the dissipation of solar radiation by the surface results in convective turbulence that mixes scalars (CO_2, H_2O, heat, momentum, etc.) from the surface to the top of the ABL. As convection slows towards the day's end, a stable nocturnal boundary layer begins to build at the earth's surface. Overlying the nocturnal boundary layer is the residual boundary layer – a remnant of the previous day's CBL – which is separated from the nocturnal boundary layer below and the free troposphere above by discontinuities in density. As convection resumes after sunrise, the residual boundary layer and nocturnal boundary layer rapidly mix to a homogenous CBL. Viewed in this way, the ABL defines an air mass that may accumulate scalars over several days.

The mixing ratio of scalars in the ABL is influenced by the interaction of several processes, the relative balance of which may change dramatically over the synoptic cycle or with the initiation of deep convection (Freedman *et al.*, 2001). Under high-

pressure systems, surface evaporation of water moistens the ABL. This is opposed by subsidence of dry air from the free troposphere, divergent flow of the ABL in the horizontal and by the formation of boundary layer clouds (Fitzjarrold, 2002). CO_2 and other scalars are similarly influenced by their surface fluxes and the mass flux of air from the free troposphere through the ABL (Betts *et al.*, 2004). During low pressure, or upon initiation of strong convection, there may be convergent flow in the horizontal, coupled with deep, precipitating convection (Stull, 1988). Cotton *et al.*, (1995) calculate that the ABL volume is, on average, turned over by deep convection every four days. Down-drafts, associated with evaporation of precipitation into free-tropospheric air, during storms and frontal passages can replace the ABL air mass with cool, moist air and reset the concentration of other scalars to that of the free troposphere (Hurwitz *et al.*, 2004). *Figure 1* illustrates these processes on a variety of temporal scales. Individual, clear weather days show strong gradients in $[CO_2]$ (C, parts per million, p.p.m.) and $[H_2O]$ (q) between the ABL (C_m, q_m) and the free troposphere (C_t, q_t) and also clearly demarcate the inversion at the ABL top (*Figure 1a, b*). The data in *Figure 1a, b* were collected directly by airplane during one afternoon under fair-weather or high-pressure conditions. As storm fronts pass, ABL air can rapidly be replaced by free-tropospheric air. In *Figure 1c*, C_m changed more than 20 p.p.m. in less than a minute owing to strong vertical mixing associated with storm downdrafts. *Figure 1d* shows two frontal sequences where $[CO_2]$ slowly declines in the ABL during high pressure conditions and then approaches free troposphere $[CO_2]$ when a low pressure system passes through the area. On longer time scales, high pressure systems are temporally dominant such that when the averaging period of $[CO_2]$ in the ABL and the free troposphere is increased, we see differences that are suggestive of the seasonally predominant surface flux; photosynthesis in summer and respiration in fall, winter, and spring (*Figure 1e, f*).

The ABL represents a large volume that typically moves across the land surface about 500 km d^{-1} (Raupach *et al.*, 1992). Therefore, studies of the ABL CO_2 balance have the potential to provide information on carbon balance of the land surface on a regional-scale. Estimates of the surface area of integration by the ABL range from 10^4 to 10^6 km^2 (Gloor *et al.*, 2001; Raupach *et al.*, 1992). Several studies have used CO_2 budgets in the ABL to estimate regional, net surface flux of CO_2 during the daytime when the full, mixed ABL is coupled to the surface and the overlying free-troposphere (Denmead *et al.*, 1996; Kuck *et al.*, 2000; Levy *et al.*, 1999; Lloyd *et al.*, 2001; Styles *et al.*, 2002). These studies have demonstrated that budget methods for the period of daytime boundary layer growth can be used to obtain estimates of daytime surface fluxes. However, the difficulty in quantifying fair-weather cloud flux, entrainment, subsidence, and horizontal divergence over a day results in widely variable agreement between ABL budget methods and surface-based methods (Fitzjarrald, 2002). Additionally, the ABL is decoupled from the surface at night, which complicates boundary layer budget closure over complete diurnal cycles. Taken together, these difficulties make the standard boundary layer budget approach impractical for long-term CO_2 balance estimates.

To obtain longer-term estimates of net CO_2 flux at the integrative ABL scale, we make a sharp break from previous CO_2 budget attempts. The ABL is an integral component in large-scale circulation as it connects the ascending and descending branches of the atmospheric circulation. Here we assume that the properties of the ABL

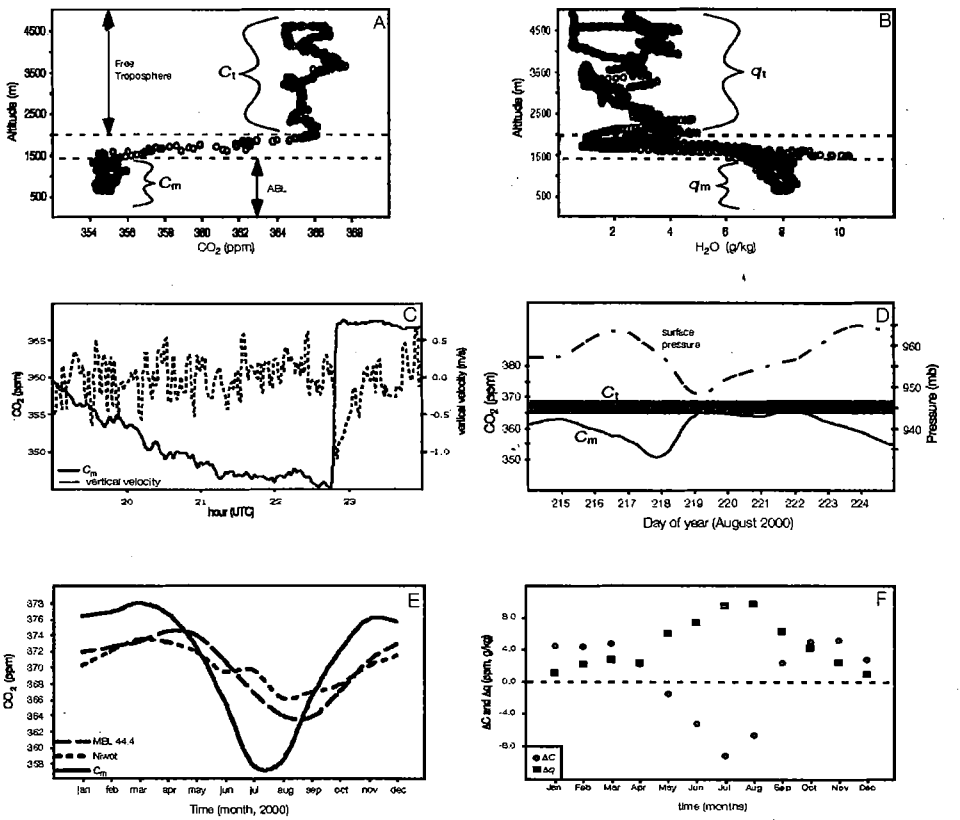

Figure 1. *Representative ABL profiles of (a) $[CO_2]$ and (b) $[H_2O]$ during mid-afternoon. Data were obtained directly by airplane in August 2000 by the COBRA campaign. (c) Five hour period of $[CO_2]$ (solid line) and vertical velocity (dashed line) measured at 396 m from the WLEF tower. (d) $[CO_2]$ (solid line) and surface pressure (dash-dot line) for several days of August 2000 at the WLEF tower site. C_m values are 24 h averages of $[CO_2]$ at 396 m. The dashed line and shaded area represent the mean free-tropospheric CO_2 mixing ratio and standard deviation for all of August (measured directly by COBRA). (e) Monthly averages of $[CO_2]$ in the marine boundary layer (MBL) at 44.4° N, from 3475 m from atop Niwot Ridge, CO, 40.1° N, and from 396 m from the WLEF tower, 45.9° N (C_m). (f) Monthly averages of ΔC ($C_t - C_m$; open circles) and Δq ($q_t - q_m$; closed squares) for the year 2000. C_m and q_m were obtained through continuous measurements at 396 m from the tower. C_t was obtained by monthly averages of $[CO_2]$ collected at Niwot Ridge, CO. RUC weather-forecasting data from the geopotential heights of 3200–7600 m were used to obtain q_t. Data for figure (c) are from Hurwitz et al. (2004). Data from (d) and (e) are from Helliker et al. (2004).*

approach a steady-state or equilibrium between the surface fluxes, cloud effects on radiation and subsidence of the overlying free troposphere over temporal scales longer than a day; an equilibrium which is controlled by larger scale processes that influence air mass ascension (low-pressure systems) and subsidence (high-pressure

systems). The equilibrium assumption is a fundamental shift from the focus on the dynamics of the diurnal cycle of the ABL to the slow evolution of the ABL, averaged over the diurnal cycle, and for much of the time nearly in balance with larger-scale subsiding circulations. The non-linear processes of daytime ABL growth and the decoupling of the stable boundary layer at night are superimposed on this slowly evolving mean state.

The concept of an 'equilibrium boundary layer' was first put forth by Betts and Ridgeway (1989) for the marine boundary layer over the open ocean and later applied to land by Betts (2000, 2004) and Betts *et al.* (2004). Betts (2000) observed that the equilibrium boundary layer approach adequately explained the observed water vapor, potential temperature, and boundary layer height of composites representing several synoptic cycles. Betts *et al.* (2004) extended the idealized model of Betts (2000) to show how the mixed layer equilibrium of water vapor, CO_2, and radon was coupled to surface fluxes through mass exchange with the free troposphere during periods of large-scale subsidence. Betts (2004) showed that the 24 hour mean climatic state and fluxes describe the coupling over land using 30 years of the fully time-dependent, European Center for Medium-Range Weather Forecasting (ECMWF) reanalysis model data. Helliker *et al.*, (2004) extended the equilibrium approach to observations of CO_2 and H_2O flux and mixing ratio data. By using observed, long-term averages of H_2O flux and mixing ratio data, they solved for an observation-based estimate of mass exchange of the ABL with the free troposphere. This estimate of mass exchange was then used to estimate the average net surface flux of CO_2 on monthly to annual periods. Further support of the equilibrium assumption was obtained by Bakwin *et al.* (2004) who showed that monthly surface fluxes could be recovered by applying model estimates of vertical exchange to observations of long-term, average differences in CO_2 between the ABL and the free troposphere.

3. Equilibrium atmospheric boundary layer CO_2 flux method

In this section, we outline the underlying equations and discuss some results for equilibrium CO_2 flux in the ABL. The study site was located in sparsely populated, north-central Wisconsin, USA, and the study platform was the 447 m tall WLEF (WLEF are the national public broadcast station call letters) television broadcast tower from which continuous [CO_2], [H_2O], and EC measurements have been made since 1995 (Bakwin *et al.*, 1998; Davis *et al.*, 2003). The tower is located within the Chequamegon-Nicolet National Forest and is a National Ocean and Atmospheric Administration-Climate Monitoring and Diagnostics Lab. (NOAA-CMDL) CO_2 sampling site (Bakwin *et al.*, 1998). The area is largely forested for hundreds of kilometers to the east and west, Lake Superior is approximately 70 km to the north and agriculture begins to dominate about 200 km to the south. The dominant forest types are mixed northern hardwood, aspen, and wetlands.

The tower measurement height of 396 m is well within the convective boundary layer during the day and typically within the residual layer and above the stable nocturnal boundary layer at night. Over a composite diurnal cycle, the CO_2 mixing ratio measured at 396 m typically varies little as compared to measurements at 30 m (Yi *et al.*, 2001). Thus, continuous measurements from this height reflect changes in the daytime convective boundary layer and the night-time residual layer through time

$\partial C_m/\partial t$. Cotton *et al.* (1995) showed that on a global average ABL air is replaced by free-tropospheric air every four days, so on these longer timescales, we assume that horizontal advection becomes less important than vertical advection and mixing across the substantial jump in $[CO_2]$ associated with the capping inversion of the ABL. We therefore use a simplified budget equation for the ABL with depth z and mean $[CO_2]$ C_m in which we neglect horizontal advection. As the ABL deepens in a subsiding mean flow ($\overline{w_+}$) it entrains air from the free troposphere above with properties C_t, and we can write the budget equation for the ABL as (Betts, 1992; Helliker *et al.*, 2004):

$$\frac{\partial}{\partial t}(\rho z C_m) = F_{NEE} + \rho\left(\frac{\partial z}{\partial t}\right) C_t - \rho w_+ (C_t - C_m) \tag{1}$$

where F_{NEE} is the net surface CO_2 flux (including photosynthetic uptake, respiratory and fossil-fuel release) in flux density units (μmol m^{-2} s^{-1}). Rearranging and ignoring the time variation of the molar mean air density, ρ, gives

$$\rho z \frac{\partial C_m}{\partial t} = F_{NEE} - \rho w (C_t - C_m) \tag{2}$$

where $w = \left(\frac{\partial z}{\partial t}\right) - \overline{w_+}$ is the entrainment rate of the ABL, or the rate at which the ABL mixes in air from the free troposphere (i.e., $\overline{w_+}$) is typically negative corresponding to mean subsidence. In strict equilibrium, $\frac{\partial C_m}{\partial t} = \frac{\partial h}{\partial t} = 0$ and we get

$$F_{NEE} = \rho w (C_t - C_m) = \rho \overline{w_+} (C_t - C_m). \tag{3}$$

A similar equation to (2) can be written for water vapour, and following the same assumptions and derivation we arrive at

$$\rho z \frac{\partial q_m}{\partial t} = F_q - \rho w (q_t - q_m) \tag{4}$$

and

$$F_q = \rho w (C_t - C_m). \tag{5}$$

Note that over longer averaging periods, the time rate of change terms $\left(\frac{\partial C_m}{\partial t}, \frac{\partial q_m}{\partial t}\right)$ become small compared with the flux terms (Helliker *et al.*, 2004). Following Raupach *et al.* (1992), we assume similarity of transport for C and q. Using long-term averages of observed F_q and $(q_t - q_m)$ and rearranging equation (5) to solve for ρw, we can obtain the observation-based estimate of vertical exchange over the given averaging period. ρw thus obtained can then be used along with observed difference in ABL-to-free-troposphere $[CO_2]$ (for example, from *Figure 1f*) to solve for F_{NEE} through equation (3).

Precipitation and subsequent evaporation processes violate the assumption of similar transport for CO_2 and water vapour, so we filtered data to exclude days when precipitation was more than 1 mm (precipitation (ppt) < 1). However, subsidence-dominant (fair-weather) days are temporally dominant, so we also present data that

represent complete monthly averages with no rainy days removed (all days). Monthly estimates of NEE using periods when precipitation days are omitted and periods using all data (thus including periods when low pressure systems pass through the area) are presented in *Figure* 2. F_{NEE} was determined by equation (3) using two independent estimates of ρw: our observation-based, flux-difference estimate ($F_{NEE\text{-}FD}$) and the estimate obtained from the NCEP/NCAR reanalysis model data ($F_{NEE\text{-}\Omega}$). EC estimates of NEE (N_{EC}) measured from the WLEF tower at 122 m are also presented in *Figure* 2. There was remarkable agreement between the independent estimates of NEE. All estimates of NEE showed similar sink-to-source phase shifts and there was good agreement between the estimates on a monthly basis. The overall agreement between the various methods for calculating F_{NEE} and N_{EC} shows that, on longer time scales, the vertical flux of CO_2 from the free troposphere is in near balance with the net CO_2 flux at the surface and the assumptions of the equilibrium ABL appear to be valid.

For all methods of calculating F_{NEE}, $F_{NEE\text{-}FD}$ (all days) had the largest propagated errors (bars shown in *Figure 2*). The errors were relatively small, but they should be considered incomplete as we had to make several assumptions in calculating F_{NEE} and the error associated with these assumptions is not currently quantifiable. First, proxies rather than direct measurements had to be used for C_t and q_t. For C_t we assumed that on a monthly basis, $[CO_2]$ measured in the marine boundary layer, at a similar latitude as the WLEF tower, was representative of mean $[CO_2]$ in the free

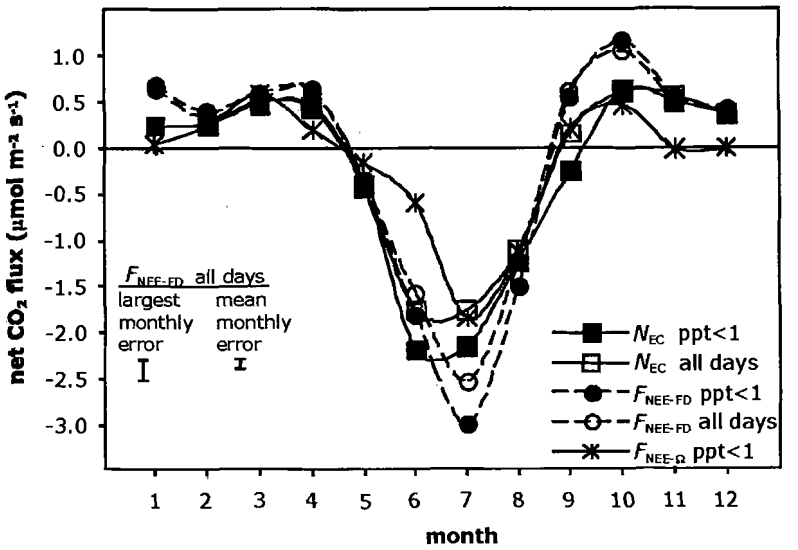

Figure 2. *Net ecosystem exchange for CO_2 (NEE) as determined by equation (3) using our flux-difference method with water vapour ($F_{NEE\text{-}FD}$), using equation (3) and NCEP/NCAR reanalysis data for ρw ($F_{NEE\text{-}\Omega}$) and from EC estimates (N_{EC}). For $F_{NEE\text{-}FD}$ and N_{EC} estimates are given for all days in a month and $F_{NEE\text{-}FD}$, N_{EC}, and $F_{NEE\text{-}\Omega}$ estimates are presented with the precipitation filter to remove days with more than 1 mm of precipitation (ppt < 1). $F_{NEE\text{-}FD}$ was calculated using C_t from the MBL (Figure 1e). q_t was obtained from RUC data. F_q, C_m and q_m were obtained by averaging the 24 h observations from the WLEF tower for a given month.*

troposphere above Wisconsin (Helliker *et al.*, 2004). For q_t, we had to use monthly averages of model outputs for water vapour from the heights of 2500–3200 m above ground level (rapid update cycle short-range weather forecasting model, http://maps.fsl.noaa.gov/). Second, we assumed that F_q measured by EC at 122 m was fairly representative of the region for calculating ρw through equation (5). For future applications, it would be ideal to have regular flights to build monthly estimates of C_t and q_t from direct measurements. These measurements are currently planned under the implementation of the North American Carbon Plan (Wofsy and Harris, 2002). We obviously need larger estimates of surface water vapour flux than EC measurements provide, and there are more robust land-coverage-based methods for estimating the largely unidirectional flux of water vapour for future tests of the flux-difference method (Anderson *et al.*, 1997, 2000; Mackay *et al.*, 2002). Finally, we do not explicitly include fossil fuel emissions in our regional analysis, but the surface footprint that affects C_m could include a larger fossil fuel flux component than the eddy correlation footprint. It is possible that the differences between $F_{NEE\text{-}FD}$ and N_{EC} reflect different fossil fuel emissions within the different footprints. Further study using the direct measurements mentioned above, together with measurements of stable isotopes, are required to quantify these flux differences.

4. Isotopes in the equilibrium atmospheric boundary layer

The analysis of naturally occurring stable isotopes in plant material provides invaluable insight into integrated plant processes (Farquhar *et al.*, 1989). As a corollary, the effect that plants have on the stable isotopes of CO_2 of atmospheric air offers an integration of surface flux processes (Ehleringer *et al.*, 2002; Lloyd *et al.*, 1996; Yakir and Sternberg 2000). Plant and ecosystem responses to short- and long-term climatic changes can be assessed by the analysis of carbon and oxygen isotopes. At ecosystem and larger scales the distinct isotopic signature associated with photosynthesis and respiration allows for the partitioning of NEE into its primary components (Bowling *et al.*, 2001; Bowling *et al.*, 2003; Lloyd *et al.*, 1996; Ogée *et al.*, 2004; Yakir and Wang, 1996). In this section, we use the equilibrium or steady-state assumptions from above to (i) develop the theory behind net isotope effects in an equilibrium boundary layer, (ii) examine some estimates of net carbon isotope composition ($\delta^{13}C_{net}$) for an entire year and, (iii) examine a flux partitioning exercise with measurements of oxygen isotope ratios ($\delta^{18}O$).

As others have defined, the NEE of CO_2 can be represented by

$$F_{NEE} = F_p + F_r \tag{6}$$

where F_p and F_r are the ABL-scale gross fluxes of CO_2 uptake (photosynthesis) and release (respiration and fossil fuel at the ABL scale), respectively. From equations (3) and (6), we can write the following equality:

$$F_{NEE} = \rho w\,(C_t - C_m) = F_p + F_r. \tag{7}$$

For any stable isotope pair, the major isotope (such as ^{12}C or ^{16}O) is in such excess that abundance is directly proportional to concentration as measured from an infra-red

gas analyser system. When the stable isotope composition is measured simultaneously, and if we know the magnitude of the fractionations that occur against the heavy isotope (^{13}C or ^{18}O), then we can calculate the relative contribution by isotopic mass balance – for absolute concentrations or fluxes of CO_2 from photosynthesis or respiration. Thus, the measured net isotope composition will reflect the sum of constituent components, and for any heavy isotope we can write,

$$F_{NEE}\delta_{net} = \rho w\,(C_t\delta_t - C_m\delta_m) \tag{8}$$

and

$$F_{NEE}\delta_{net} = F_p\delta_p + F_r\delta_r \tag{9}$$

where δ values are the isotope ratio of an associated CO_2 flux or mixing ratio expressed relative to a standard by,

$$\delta = \left(\frac{R_{sample}}{R_{standard}} - 1\right) 1000 \tag{10}$$

where R is the molar ratio of heavy to light isotopes ($^{13}C : {}^{12}C$, $^{18}O : {}^{16}O$). For all isotope ratios given here, the standard is Pee Dee belemnite (PDB). The term $F_{NEE}\delta_{net}$ in equations (8) and (9) is often termed the 'isoflux' (Bowling *et al.*, 2001).

By solving equation (8) for δ_{net} and recognizing from equation (3) that $F_{NEE}/\rho w = (C_t - C_m)$ we obtain

$$\delta_{net} = \frac{(C_t\delta_t - C_m\delta_m)}{(C_t - C_m)} \tag{11}$$

which explains δ_{net} based solely on the equilibrium differences in CO_2 and isotopes between the ABL and the overlying free troposphere. Equation (11) is the 'delta-notation' form of the equation derived by Farquhar in Evans *et al.* (1986) for measurement of on-line isotope discrimination. Note that equation (11) allows for the estimation of δ_{net} independently of any knowledge of surface flux.

By solving (9) for δ_{net} and inserting (6) we obtain

$$\delta_{net} = \frac{F_p\delta_p + F_r\delta_r}{F_p + F_r} \tag{12}$$

which explains δ_{net} based on the individual surface flux components. δ_{net} can further be expressed as a function of the ratio of photosynthetic uptake to CO_2 release, γ ($\gamma = F_p/F_r$) and inserted into equation (12):

$$\delta_{net} = \frac{\delta_r}{1+\gamma} + \frac{\delta_p\gamma}{1+\gamma} \tag{13}$$

δ_{net} can be obtained through equation (11) with average measurements of the mixing and isotope ratios of ABL and free-tropospheric CO_2. δ_r can be estimated by Keeling plot analysis (Flanagan *et al.*, 1996; Keeling, 1958) and, by knowing the environmental inputs, δ_p can be modelled (Farquhar *et al.*, 1993; Flanagan *et al.*, 1994; Gillon and Yakir, 2000). Hence, by knowing all the isotopic inputs at the ABL-scale and

re-arranging equations (12) or (13), we can partition F_{NEE} into the component parts of photosynthesis and respiration in a similar manner to the approaches used at the ecosystem scale (Bowling *et al.*, 2001, 2003; Ogée *et al.*, 2004; Yakir and Wang, 1996).

Figure 3a shows monthly averages of the $\delta^{13}C$ of CO_2 measured at the WLEF tower and from Niwot Ridge ($\delta^{13}C_t$), a mountain top in Colorado, USA. Both sites are part of the NOAA-CMDL flask collection program (Globalview-CO_2, 2003). The $\delta^{13}C$ of ABL CO_2 ($\delta^{13}C_m$) was heavier than the free-tropospheric proxy ($\delta^{13}C_t$) in the summer (i.e., enriched in ^{13}C) and lighter in the winter (i.e., depleted in ^{13}C). Similar to the CO_2 mixing ratio measurements, this pattern is consistent with the predominance of photosynthetic discrimination against ^{13}C in the summer and the respiratory release of CO_2, depleted in ^{13}C, in the winter. Estimations of δ_{net} are shown in *Figure 3b*. For the summer months δ_{net} ranged from –23.3 to –25.2 and was very consistent for July and August. For May, September, and October, the values of δ_{net} varied widely as the differences in CO_2 between the ABL and free troposphere were small. These seemingly odd values of δ_{net} are expected as $\gamma \rightarrow 1$ during the seasonal transition from CO_2 sink to source (Miller and Tans, 2002). During the winter, δ_{net} was very negative, possibly reflecting fossil-fuel inputs that would become proportionally larger during the winter months and have isotope ratios that are typically lighter than that of biospheric exchange.

Knowledge of the net flux of CO_2 and δ_{net} for each month can be used to calculate the corresponding flux-weighted isotopic signature associated with the yearly net uptake of CO_2 by this region. This value, which was –9.5‰, may be somewhat surprising because northern Wisconsin is a C_3-dominated region, and carbon fixed by C_3 plants typically has a $\delta^{13}C$ closer to –25‰. However, this apparent discrepancy can be explained if there is an offset between respiration and photosynthesis (i.e., the isotopic composition of carbon fixed is not equal to that respired and $\gamma \approx 1$ for the year (Miller and Tans, 2002)). To illustrate, we offer a sample calculation of the isotopic composition of the gross CO_2 release (δ_r) that would be required to satisfy the mass and isotope balance of equation (13). It was assumed that $\gamma = -1.03$ and that the isotopic composition of carbon taken up by gross photosynthesis, $\delta_p = -25‰$. The calculation indicates that a value of $\delta_r = -25.5‰$ would satisfy the seasonal net storage of –9.5‰. This might occur, for example, if the gross CO_2 released was 90% from biological decomposition with $\delta_R = -25.0‰$ and 10% from fossil fuel combustion with $\delta_{ff} = -29.6‰$. Additionally, the disequilibrium caused by fossil fuel inputs might explain the distinct seasonal pattern in the observed δ_{net} (*Figure 3b*), where the values were considerably more negative in the winter months than in the summer months.

Recent analysis has shown that oxygen isotopes are preferred over carbon isotopes to partition ecosystem fluxes because the differences in isotope ratio between respiration and photosynthesis are considerably larger and result in smaller uncertainties around the partitioned fluxes (Ogée *et al.*, 2004). For a second partitioning exercise we use oxygen isotopes and capitalize on a two-day period in August 2000 when we had direct measurements of ABL and free-tropospheric [CO_2] through the CO_2 Budget and Regional Airborne study (COBRA) campaign (Gerbig *et al.*, 2003). During this period we were able to measure δ_{net}, δ_r, and model δ_p to solve for γ (*Table 1*). We then used γ and estimates of NEE to partition fluxes into photosynthesis and respiration. For this period, we assumed that the fossil-fuel flux was small compared with the size of photosynthetic and respiratory fluxes. Our results for the

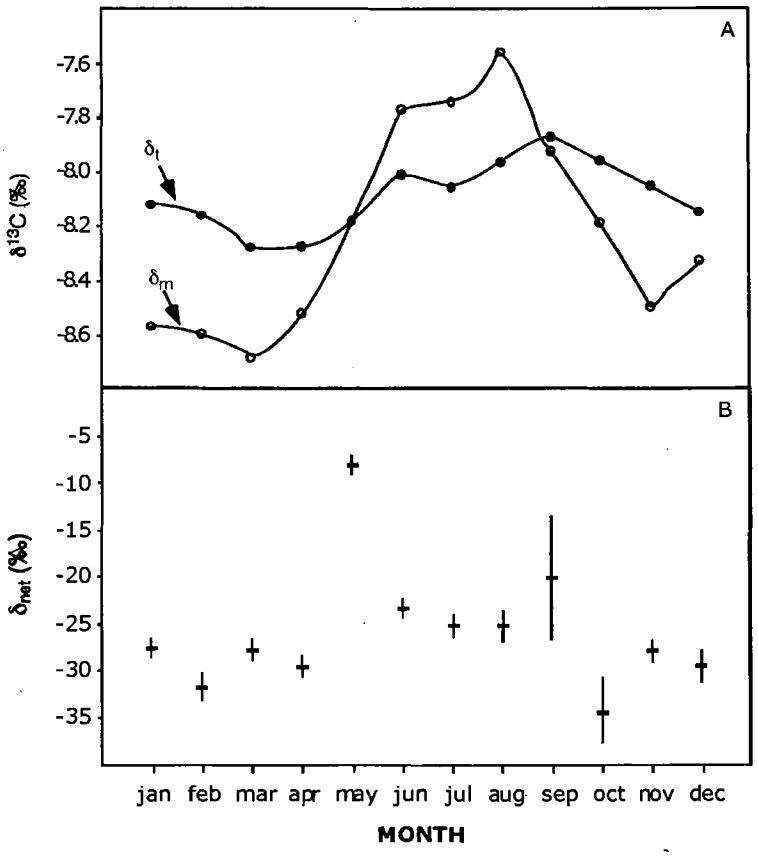

Figure 3. *(a) Monthly averages of the $\delta^{13}C$ of CO_2 measured at the WLEF tower ($\delta^{13}C_m$) and from Niwot Ridge ($\delta^{13}C_i$). (b) δ_{net} calculated through equation (11) using isotope ratios in (a) and CO_2 mixing ratios from Figure 1e. The vertical lines represent the propagated error for the calculation of δ_{net}*

partitioned fluxes agreed with independent estimates of flux partitioning through EC-based techniques (*Table 1*). The errors around our estimates are fairly large, but they are comparable to other, accepted methods of flux partitioning. For both of the partitioning exercises detailed here, the input parameters need to be better constrained by measurements before the results of such calculations can be taken seriously. However, this illustrates the additional power that an isotope budget can provide in studies of net carbon exchange.

5. Conclusions

By approaching monthly average CO_2 and water vapour mixing ratios in the ABL as an equilibrium problem, we estimated net CO_2 surface exchange over a forested region for an entire year. These ABL-scale net CO_2 estimates were comparable to measurements made by EC over this same time period. These experiments lend

Table 1. *ABL-scale flux partitioning exercise using stable oxygen isotopes.*

				ABL-scale estimates			Eddy covariance estimates	
δ_{net} (‰)	δ_r (‰)	δ_p (‰)	γ	NEE (μmol m^{-2} s^{-1})	F_p (μmol m^{-2} s^{-1})	F_r (μmol m^{-2} s^{-1})	F_p (μmol m^{-2} s^{-1})	F_r (μmol m^{-2} s^{-1})
−1.9	−13.5	−11.4	−1.2	−1.2	−6.7	5.5	−7.1	5.9
±0.9	±1.4	±1.3	±0.2		±1.3	±1.3	±1.1	±1.1

observational support to the underlying equilibrium hypothesis that over long averaging periods, and during periods of subsidence, the surface flux of CO_2 and water vapour into the ABL are at a near-balance with the mixing-down of air from the free troposphere.

The individual manner in which gross carbon fluxes of photosynthesis, respiration, and fossil fuel use respond to short- and long-term climatic change has large effects on the global carbon cycle. Stable isotopes have been shown to be invaluable tracers of these gross carbon flux processes at leaf, ecosystem, and global scales. However, the uncertainty of these gross processes on the global scale is large because of the lack of knowledge in how leaf-level and ecosystem-level processes play out on regional scales, and how the regional modification of the isotopes in atmospheric CO_2 affect the observations at the global scale. By applying the ABL equilibrium concepts to the measurement of stable isotopes in the ABL and free troposphere, we were able to estimate the regional isotope effects and obtain reasonable estimates of the gross fluxes of CO_2, thus closing a major gap in scales in our current observations.

The ABL flux-difference method presented here can be improved with more systematic mixing ratio and isotope ratio data collection, and more rigorous uncertainty analysis. With these improvements in the method and with more sampling sites, it is not unreasonable to propose that this method could be extended to obtain not only regional, but continental-scale measurements of CO_2 and isotope flux. These improvements have the potential to give us an independent estimate of carbon sources and sinks on an annual basis and help resolve some of the outstanding questions concerning the carbon cycle in forested regions.

References

Anderson, M.C., Norman, J.M., Diak, G.R., Kustas, W.P. and Mecikalski, J.R. (1997) A two-source time-integrated model for estimating surface fluxes using thermal infrared remote sensing. *Remote Sensing of Environment* **60:** 195–216.

Anderson, M.C., Norman, J.M., Meyers, T.P. and Diak, G.R. (2000) An analytical model for estimating canopy transpiration and carbon assimilation fluxes based on canopy light-use efficiency. *Agricultural and Forest Meteorology* **101:** 265–289.

Bakwin, P.S., Tans, P.P., Hurst, D.F. and Zhao, C. (1998) Measurements of carbon dioxide on very tall towers: results of the NOAA/CMDL program. *Tellus Series B – Chemical and Physical Meteorology* **50:** 401–415.

Bakwin, P.S., Davis, K.J., Yi, C., Wofsy, S.C., Munger, J.W., Haszpra, L. and Barcza, Z. (2004) Regional carbon dioxide fluxes from mixing ratio data. *Tellus Series B – Chemical and Physical Meteorology* **56:** 301–311.

Baldocchi, D., Falge, E., Gu, L.H., Olson, R., Hollinger, D., Running, S. *et al.* (2001) FLUXNET: A new tool to study the temporal and spatial variability of ecosystem-scale carbon dioxide, water vapor and energy flux densities. *Bulletin of the American Meteorological Society* **82:** 2415–2434.

Battle, M., Bender, M.L., Tans, P.P., White, J.W.C., Ellis, J.T., Conway, T. and Francey, R.J. (2000) Global carbon sinks and their variability inferred from atmospheric O_2 and $\delta^{13}C$. *Science* **287:** 2467–2470.

Betts, A.K. (1992), FIFE Atmosheric Boundary Layer Budget Methods. *J. Geophys. Res.*, **97:** 18523–189532.

Betts, A.K. (2000) Idealized model for equilibrium boundary layer over land. *Journal of Hydrometeorology* **1:** 507–523.

Betts, A.K. (2004) Understanding hydrometeorology using global models. American Meteorological Society Robert E. Horton Lecture. *Bulletin of the American Meteorological Society* in press.

Betts, A.K. and Ridgway, W.L. (1989) Climatic equilibrium of the atmospheric convective boundary layer over a tropical ocean. *Journal of Atmospheric Sciences* **46:** 2621–2641.

Betts, A.K., Helliker, B.R. and Berry, J.A. (2004) Coupling between CO_2, water vapor, temperature and radon and their fluxes in an idealized equilibrium boundary layer over land. *Journal of Geophysical Research – Atmospheres.* In press.

Bousquet, P., Ciais, P., Peylin, P., Ramonet, M. and Monfray, P. (1999) Inverse modeling of annual atmospheric CO_2 sources and sinks: I. Method and control inversion. *Journal of Geophysical Research,* **104:** 26161–26178.

Bowling, D.R., Tans, P.P. and Monson, R.K. (2001) Partitioning net ecosystem carbon exchanges with isotopic fluxes of CO_2. *Global Change Biology* **7:** 127–145.

Bowling, D.R., Pataki, D.E. and Ehleringer, J.R. (2003) Critical evalutation of micrometeorological methods for measuring ecosystem–atmosphere isotopic exchange of CO_2. *Agricultural and Forest Meteorology* **116:** 159–179.

Ciais, P., Tans, P.P., Trolier, M., White, J.W.C. and Francey, R.J. (1995) A large Northern Hemisphere terrestrial CO_2 sink indicated by the $^{13}C/^{12}C$ ratio of atmospheric CO_2. *Science* **269:** 1098–1102.

Cotton, W.R., Alexander, G.D., Hertenstein, R., Walko, R.L., McAnelly, R.L. and Nicholls, M. (1995) Cloud venting – a review and some new global annual estimates. *Earth-Science Reviews* **39:** 169–206.

Davis, K.J., Bakwin, P.S., Berger, B.W., Yi, C., Zhao, C., Teclaw, R.M. and Isebrands, J.G. (2003) Long-term carbon dioxide fluxes from a very tall tower in a northern forest: Annual cycle of CO_2 exhange. *Global Change Biology* **9:** 1278–1293.

Denmead, O.T., Raupach, M.R., Danin, F.X., Cleugh, H.A. and Leuning, R. (1996) Boundary layer budgets for regional estimates of scalar fluxes. *Global Change Biology* **2:** 275–285.

Ehleringer, J.R., Bowling, D.R., Flanagan, L.B., Fessenden, J., Helliker, B.R., Martinelli, L.A. and Ometto, J.P. (2002), Stable isotopes and carbon cycle processes in forest and grasslands. *Plant Biology* **4:** 181–189.

Evans, J.R., Sharkey, T.D., Berry, J.A. and Farquhar, G.D. (1986) Carbon isotope discrimination measured concurrently with gas exchange to investigate CO_2 diffusion in leaves of higher plants. *Australian Journal of Plant Physiology* **13:** 281–292.

Fan, S., Gloor, M., Mahlman, J., Pacala, S., Sarmiento, J., Takahashi, T. and Tans, P. (1998) A large terrestrial carbon sink in North America implied by atmospheric and oceanic carbon dioxide data and models. *Science* **282:** 442–446.

Farquhar, G.D., Ehleringer, J.R. and Hubick, K.T. (1989) Carbon isotope discrimination and photosynthesis. *Annual Review of Plant Physiology and Plant Molecular Biology* 40: 503–537.

Farquhar, G.D., Lloyd, J., Taylor, J.A., Flanagan, L.B., Syvertsen, J.P., Hubick, K.T., Wong, S.C. and Ehleringer, J.R. (1993) Vegetation effects on the isotope composition of oxygen in atmospheric CO_2. *Nature* **363:** 439–443.

Fitzjarrald, D.R. (2002) Boundary layer budgeting. In: Kabat, P., Claussen, M., Dirmeyer, P.A., Gash, J.H., Bravo de Guennin, C., Meybeck, L. *et al.* (eds) *Vegetation, Water, Humans and the Climate: A new Perspective on an Interactive System.* Springer-Verlag, New York, pp. 239–254.

Flanagan, L.B., Brooks, J.R., Varney, G.T., Berry, S.C. and Ehleringer, J.R. (1996) Carbon isotope discrimination during photosynthesis and the isotope ratio of respired CO_2 in boreal forest ecosystems. *Global Biogeochemical Cycles* 10: 629–640.

Flanagan, L.B., Phillips, S.L., Ehleringer, J.R., Lloyd, J. and Farquhar, G.D. (1996) Effect of changes in leaf water oxygen isotopic composition on discrimination against $C^{18}O^{16}O$ during photosynthetic gas exchange. *Australian Journal of Plant Physiology* **21:** 221–234.

Freedman, J.M., Fitzjarrald, D.R., Moore, K.E. and Sakai, R.K. (2001) Boundary layer clouds and vegetation–atmosphere feedbacks. *Journal of Climate* 14: 180–197.

Gerbig, C., Lin, J.C., Wofsy, S.C., Daube, B.C., Andrews, A.E., Stephens, B.B., Bakwin, P.S. and Grainger, A. (2003) Toward constraining regional-scale fluxes of CO_2 with atmospheric observations over a continent: 1. Observed spatial variability from airborne platforms. *Journal of Geophysical Research* **108:** doi:10.1029/2002JDOO3 018.

Gillon, J.S. and Yakir, D. (2000) Internal conductance to CO_2 diffusion and $C^{18}OO$ discrimination in C3 leaves. *Plant Physiology* **123:** 201–213.

Globalview-CO_2 (2003) Cooperative Atmospheric Data Integration Project – Carbon Dioxide. CD-ROM, NOAA/CMDL, Boulder, Colorado. (Also available on Internet via anonymous FTP at ftp.cmdl.noaa.gov, Path: ccg/co2/GLOBALVIEW).

Gloor, M., Bakwin, P., Hurst, D., Lock, L., Draxler, R. and Tans, P. (2001) What is the concentration footprint of a tall tower? *Journal of Geophysical Research* **106:** 17831–17840.

Goodale, C.L., Apps, M.J., Birdsey, R.A., Field, C.B., Heath, J.S., Houghton, J.C. *et al.* (2002) Forest carbon sinks in the Northern Hemisphere. *Ecological Applications* 12: 891–899.

Helliker, B.R., Berry, J.A., Betts, A.K., Davis, K., Miller, J., Denning, A.S., Bakwin, P., Ehleringer, J., Butler, M.P. and Ricciuto, D. (2004) Estimates of net CO_2 flux by application of equilibrium boundary layer concepts to CO_2 and water vapor measurements from a tall tower. *Journal of Geophysical Research – Atmospheres* In press.

Hurwitz, M.D., Ricciuto, D.M., Davis, K.J., Wang, W., Yi, C., Butler, M.P. and Bakwin, P.S. (2004) Advection of carbon dioxide in the presence of storm systems over a northern Wisconsin forest. *Journal of Atmospheric Sciences* **61**: 607–618.

Keeling, C.D. (1958) The concentrations and isotopic abundances of atmospheric carbon dioxide in rural areas. *Geochimica et Cosmochimica Acta* **13**: 322–334.

Kuck, L.R., Smith, T., Balsley, B.B., Helmig, D., Conway, T.J., Tans, P.P. *et al.* (2000) Measurements of landscape-scale fluxes of carbon dioxide in the Peruvian Amazon by vertical profiling through the atmospheric boundary layer. *Journal of Geophysical Research* **105**: 22137–22146.

Levy, P.E., Grelle, A., Lindroth, A., Molder, M., Jarvis, P.G., Kruijt, B. and Moncrieff, J.B. (1999) Regional-scale CO_2 fluxes over central Sweden by a boundary layer budget method. *Agricultural and Forest Meteorology* **99**: 169–180.

Lloyd, J., Kruijt, B., Hollinger, D.Y., Grace, J., Francey, R.J., Wong, S.-C. *et al.* (1996) Vegetation effects on the isotopic composition of atmospheric CO_2 at local and regional scales: theoretical aspects and a comparison between rain forest in Amazonia and a boreal forest in Siberia. *Australian Journal of Plant Physiology* **23**: 371–399.

Lloyd, J., Francey, R.J., Mollicone, D., Raupach, M.R., Sogachev, A., Arneth, A. *et al.* (2001) Vertical profiles, boundary layer budgets, and regional flux estimates for CO_2 and its $^{13}C/^{12}C$ ratio and for water vapor above a forest/bog mosaic in central Siberia. *Global Biogeochemal Cycles* **15**: 267–284.

Mackay, D.S., Ahl, D.E., Ewers, B.E., Gower, S.T., Burrows, S.N., Samanta, S. and Davis, K.J. (2002) Effects of aggregated classification of forest composition on estimates of evapotranspiration in a northern Wisconsin forest. *Global Change Biology*, **8**(12): 1253–1265.

Miller, J.B. and Tans, P.P. (2002) Calculating isotopic fractionation from atmospheric measurements at various scales. *Tellus Series B – Chemical and Physical Meteorology* **55**: 207–214.

Ogée, J., Peylin, P., Cuntz, M., Bariac, T., Brunet, Y., Berbigier, P., Richard, P. and Ciais, P. (2004) Partitioning net ecosystem carbon exchange into net assimilation and respiration with canopy-scale isotopic measurements: an error propagation analysis with $^{13}CO_2$ and $CO^{18}O$ data. *Global Biogeochemical Cycles* **18** doi:10.1029/2003 GB002166.

Oren, R., Ellsworth, D.S., Johnsen, K.H., Phillips, N., Ewers, B.E., Maier, C. *et al.* (2001) Soil fertility limits carbon sequestration by forest ecosystems in a CO_2-enriched atmosphere. *Nature* **411**: 469–472.

Prentice, I.C., Farquhar, G.D., Fasham, M.J.R., Goulden, M.L., Heimann, M., Jaramillo, V.J., Kheshgi, H.S., Le Quéré, C., Scholes, R.J. and Wallace, D.W.R. (2001) The carbon cycle and atmospheric CO_2. In *Climate Change 2001: The Scientific Basis. Contribution of Working Group I to the IPCC Third Assessment Report*. Cambridge University Press. Cambride, UK.

Raupach, M.R., Denmead, O.T. and Dunin, F.X. (1992) Challenges in linking atmospheric CO_2 concentrations to fluxes at local and regional scales. *Australian Journal of Botany* **40**: 697–716.

Rayner, P.J., Enting, I.G., Francey, R.J. and Langenfelds, R. (1999) Reconstructing the recent carbon cycle from atmospheric CO_2, $d^{13}C$ and O_2/N_2 observations. *Tellus Series B – Chemical and Physical Meteorology* **51**: 213–232.

Stull, R.B. (1988) *An Introduction to Boundary Layer Meteorology*. Kluwer, Dordrecht.

Styles, J.M., Lloyd, J., Zolotoukhine, D., Lawton, K.A., Tchebakova, N., Francey, R.J., Arneth, A., Salamakho, D., Kolle, O. and Schulze, E.-D. (2002) Estimates of regional surface carbon dioxide exchange and carbon and oxygen isotope discrimination during photosynthesis from concentration profiles in the atmospheric boundary layer. *Tellus Series B – Chemical and Physical Meteorology* **54**: 768–783.

Townsend, A.R., Asner, G.P., White, J.W.C. and Tans, P. (2002) Land use effects on atmospheric ^{13}C imply a sizable terrestrial CO_2 sink in tropical latitudes. *Geophysical Research Letters* **29**: 10, doi: 10.1029/2001GL013454.

Wofsy, S.C. and Harris, R.C. (2002) *The North American Carbon Program (NACP). Report of the NACP Committee of the U.S. Interagency Carbon Cycle Science Program.* U.S. Global Change Research Program.

Yakir, D. and Sternberg, L.S.L. (2000) The use of stable isotopes to study ecosystem gas exchange. *Oecologia* **123**: 297–311.

Yakir, D. and Wang, X.F. (1996) Fluxes of CO_2 and water between terrestrial vegetation and the atmosphere estimated from isotope measurements. *Nature* **380**: 515–517.

Yi, C., Davis, K.J. and Berger, B.W. (2001) Long-term observations of the dynamics of the continental planetary boundary layer. *Journal of Atmospheric Sciences* **58**: 1288–1299.